Research Article | Vol. 9, No. 5 | 1 May 2018 | BIOMEDICAL OPTICS EXPRESS 2451
Biomedical Optics EXPRESS

Quantitative multispectral *ex vivo* optical evaluation of human ovarian tissue using spatial frequency domain imaging

SREYANKAR NANDY,[1] IAN S. HAGEMANN,[2] MATTHEW A. POWELL,[3] CARY SIEGEL,[4] AND QUING ZHU[1,4,*]

[1]*Department of Biomedical Engineering, Washington University in St. Louis, St. Louis, MO 63130, USA*
[2]*Department of Pathology and Immunology, Washington University School of Medicine, St. Louis, MO 63130, USA*
[3]*Division of Gynecologic Oncology, Department of Obstetrics and Gynecology, Washington University School of Medicine, St. Louis, MO 63110, USA*
[4]*Department of Radiology, Washington University School of Medicine, St. Louis, MO 63110, USA*
**zhu.q@wustl.edu*

Abstract: About 85-90% of all ovarian cancers are carcinomas; these manifest clinically as mass-forming epithelial proliferations involving the ovary. In this study, a visible light spatial frequency domain imaging (SFDI) system was used for multispectral *ex vivo* imaging and quantitative evaluation of freshly excised benign and malignant human ovarian tissues. A total of 14 ovaries from 11 patients undergoing oophorectomy were investigated. Using a logistic regression model with seven significant spectral and spatial features extracted from SFDI images, a sensitivity of 94.06% and specificity of 93.53% were achieved for prediction of histologically confirmed invasive carcinoma.

OCIS codes: (170.0170) Medical optics and biotechnology; (170.4440) ObGyn; (170.6935) Tissue characterization.

References and links

1. American Cancer Society, "Cancer Facts & Figures", American Cancer Society, Atlanta, Ga, USA, (2017).
2. S. Nandy, M. Sanders, and Q. Zhu, "Classification and analysis of human ovarian tissue using full field optical coherence tomography," Biomed. Opt. Express **7**(12), 5182–5187 (2016).
3. A. Aguirre, Y. Ardeshirpour, M. M. Sanders, M. Brewer, and Q. Zhu, "Potential role of coregistered photoacoustic and ultrasound imaging in ovarian cancer detection and characterization," Transl. Oncol. **4**(1), 29–37 (2011).
4. Y. Yang, X. Li, T. Wang, P. D. Kumavor, A. Aguirre, K. K. Shung, Q. Zhou, M. Sanders, M. Brewer, and Q. Zhu, "Integrated optical coherence tomography, ultrasound and photoacoustic imaging for ovarian tissue characterization," Biomed. Opt. Express **2**(9), 2551–2561 (2011).
5. D. J. Cuccia, F. Bevilacqua, A. J. Durkin, F. R. Ayers, and B. J. Tromberg, "Quantitation and mapping of tissue optical properties using modulated imaging," J. Biomed. Opt. **14**(2), 024012 (2009).
6. A. Mazhar, S. Dell, D. J. Cuccia, S. Gioux, A. J. Durkin, J. V. Frangioni, and B. J. Tromberg, "Wavelength optimization for rapid chromophore mapping using spatial frequency domain imaging," J. Biomed. Opt. **15**(6), 061716 (2010).
7. A. M. Laughney, V. Krishnaswamy, T. B. Rice, D. J. Cuccia, R. J. Barth, B. J. Tromberg, K. D. Paulsen, B. W. Pogue, and W. A. Wells, "System analysis of spatial frequency domain imaging for quantitative mapping of surgically resected breast tissues," J. Biomed. Opt. **18**(3), 036012 (2013).
8. A. M. Laughney, V. Krishnaswamy, E. J. Rizzo, M. C. Schwab, R. J. Barth, Jr., D. J. Cuccia, B. J. Tromberg, K. D. Paulsen, B. W. Pogue, and W. A. Wells, "Spectral discrimination of breast pathologies in situ using spatial frequency domain imaging," Breast Cancer Res. **15**(4), R61 (2013).
9. S. Nandy, A. Mostafa, P. D. Kumavor, M. Sanders, M. Brewer, and Q. Zhu, "Characterizing optical properties and spatial heterogeneity of human ovarian tissue using spatial frequency domain imaging," J. Biomed. Opt. **21**(10), 101402 (2016).
10. S. Gioux, A. Mazhar, D. J. Cuccia, A. J. Durkin, B. J. Tromberg, and J. V. Frangioni, "Three-dimensional surface profile intensity correction for spatially modulated imaging," J. Biomed. Opt. **14**(3), 034045 (2009).
11. S. Nandy, H. S. Salehi, T. Wang, X. Wang, M. Sanders, A. Kueck, M. Brewer, and Q. Zhu, "Correlating optical coherence elastography based strain measurements with collagen content of the human ovarian tissue," Biomed. Opt. Express **6**(10), 3806–3811 (2015).
12. S. L. Jacques, "Optical properties of biological tissues: a review," Phys. Med. Biol. **58**(11), R37–R61 (2013).

#325365 https://doi.org/10.1364/BOE.9.002451
Journal © 2018 Received 7 Mar 2018; revised 20 Apr 2018; accepted 23 Apr 2018; published 30 Apr 2018

Biomedical Optics EXPRESS

13. T. M. Bydlon, W. T. Barry, S. A. Kennedy, J. Q. Brown, J. E. Gallagher, L. G. Wilke, J. Geradts, and N. Ramanujam, "Advancing optical imaging for breast margin assessment: an analysis of excisional time, cautery, and patent blue dye on underlying sources of contrast," PLoS One **7**(12), e51418 (2012).
14. S. H. L. George, R. Garcia, and B. M. Slomovitz, "Ovarian cancer: the fallopian tube as the site of origin and opportunities for prevention," Front. Oncol. **6**, 108 (2016).

1. Introduction

Cancer of the ovary remains the deadliest of all the gynecological malignancies, accounting for over 14,000 deaths annually in the US. Due to the lack of reliable early symptoms and efficacious screening techniques, most of ovarian cancers are diagnosed at late stages (III and IV) [1]. Optical imaging modalities such as optical coherence tomography (OCT), photoacoustic imaging (PAI), have been used separately or in combination for high-resolution imaging of benign and malignant ovarian tissue microstructures [2–4]. These studies have established that absorption parameters are important biomarkers related to tumor angiogenesis and tumor metabolism, whereas, changes in the scattering properties have been found to be associated with neoplastic alterations in the ovarian collagen structure as well as tumor necrosis. Some of the limitations of these techniques include limited field of view (FOV), reduced depth sampling due to multiple scattering and discrete sampling for wide field implementation. Spatial frequency domain imaging (SFDI) is an emerging planar imaging modality that can separate optical absorption and scattering to provide large-field, depth sampled quantitative evaluation of biological tissue [5–8]. The majority (85-90%) of ovarian malignancies are epithelial cancers, many of which likely arise from Fallopian tube epithelium, and are thought to spread early to the ovary, where they then manifest clinically as expanding masses in the ovarian cortex. Previously, a single wavelength SFDI system with a bulky projection unit was used to image differences in absorption, scattering as well as spatial heterogeneities between benign and malignant ovarian tissues [9]. In the current study, we have used a multispectral SFDI system with a miniaturized projector at visible wavelengths for *ex vivo* quantification of wavelength dependent chromophores as well as spatial heterogeneities of freshly excised benign and malignant ovarian tissues. Using a logistic regression classifier, the sensitivity, specificity, positive predictive value (PPV), negative predictive value (NPV), as well as the area under the receiver operator characteristic (ROC) curve (AUC) were evaluated.

2. Materials and methods

2.1 Human ovary samples

Freshly excised ovarian tissues were collected from patients undergoing oophorectomy for suspected risk of ovarian cancer, or having an ovarian/pelvic mass suggestive of malignancy, at Washington University School of Medicine. The study was approved by the Institutional Review Board (IRB) at Washington University. Informed consent was obtained from all patients. Care was taken during the surgery to remove the ovaries intact. All imaging was completed within 1 hour of surgery. After imaging, the tissues were returned to the pathology department for histological processing.

2.2 SFDI system

Figure 1 shows the configuration of the free space SFDI system. Sinusoidal patterns generated in MATLAB were projected from a miniaturized Pico projector (RIF6 cube, dimension 2"x2"x1.9", brightness 50 lumens), and the diffuse reflected light was recorded by a 12 bit CCD camera (Basler ace, 30 fps, dynamic range 57 dB) and bandpass filters (Thorlabs, bandwidth ± 10 nm). Three wavelengths (460 nm, 530 nm and 630 nm) and two optimized spatial frequencies (0 and 1 cm^{-1}) were used for this study. The specular reflection was minimized by two crossed linear polarizers. The field of view (FOV) captured by the camera was 4 cm x 4 cm.

Biomedical Optics EXPRESS

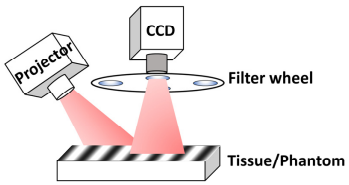

Fig. 1. SFDI system configuration.

For each wavelength, three phase shifted images (0, 120 and 240 degrees) were recorded, and the DC and AC components of the amplitude were calculated. A Monte Carlo simulation-based two-frequency lookup table was used for calculating the wide-field tissue absorption and reduced scattering maps. The system was calibrated with a known intralipid concentration (0.08%) and solid-tissue–mimicking phantoms, and both the absorption and scattering errors were within 5%. A calibration based profilometry correction was applied to account for sample surface variation [10]. The height mismatch between the reference phantom and sample was carefully adjusted to be less than 1 mm, which had negligible scaling effect on the measured diffuse reflectance.

2.3 Extraction of spectral and spatial features

Depending on the size of the ovarian mass (1.1 cm-9.5 cm), several nonoverlapping images were recorded for each sample, and subsequently each SFDI absorption and scattering image was subdivided into independent regions of interest of same size (1 cm x 1 cm, 200 x 200 pixels) for extracting the spectral and spatial features. Four features were quantitatively extracted from the observed differences between the wavelength-dependent absorption and scattering properties. These were the total hemoglobin (HbT), oxygen saturation (sO2), scatter amplitude and scatter spectral slope. HbT and sO2 are important prognosticators of angiogenesis and oxygen consumption, respectively, which are related to tumor progression. The scatter amplitude was proportional to the concentration of elastic scatterers, mainly collagen in the ovarian stroma, as established by previous studies [11]. The scatter spectral slope was related to the size of the scatterers, with higher slope indicating the presence of smaller collagen fibrils that enhanced Rayleigh-type scattering [8, 12]. Four additional features related to the heterogeneity of absorption and scattering were calculated from the SFDI images. This has been described in detail in Ref. 9. For calculating the spatial features, only a single wavelength (530 nm) was used, because the spatial features obtained from other two wavelengths were correlated and did not add more independent information.

2.4 Feature selection and classification

A two-step approach was used for classification of the different ovarian tissue types. In the first step, the features were ranked in order of decreasing p values obtained from Student's *t* test, and one feature with $p > 0.05$ was excluded from the classification. Next, a logistic regression model was trained using the MATLAB GLMFIT function with the seven significant features as predictor variables and the pathological diagnosis (1 for malignant, 0 for normal/benign) as response variables. The model was tested using GLMVAL function for estimating the response of the testing set. The receiver operating curve (ROC) and the area under the curve (AUC) were used for evaluating the accuracy of the model.

3. Results and discussions

After excluding one collapsed cystic ovary from one patient, and another two ovaries from another patient with ink on the ovary surface, we imaged a total of 14 intact ovaries (10 normal/benign, 4 malignant) from 11 patients using the SFDI system. The non-cancerous samples consisted of normal (n = 2) and enlarged but benign ovaries (n = 8). The diagnoses for the benign ovarian masses consisted of cystic ovaries and fibrothecoma. The malignant

Biomedical Optics EXPRESS

samples consisted of a borderline serous tumor (n = 1), two endometroid adenocarcinomas (n = 2) and a high-grade serous carcinoma (n = 1). Most of the benign ovaries (9 ovaries) were from post-menopausal patients, while all the malignant ovaries were from pre-menopausal patients. The borderline tumor was included in the malignant category due to the clinical impact of this diagnosis.

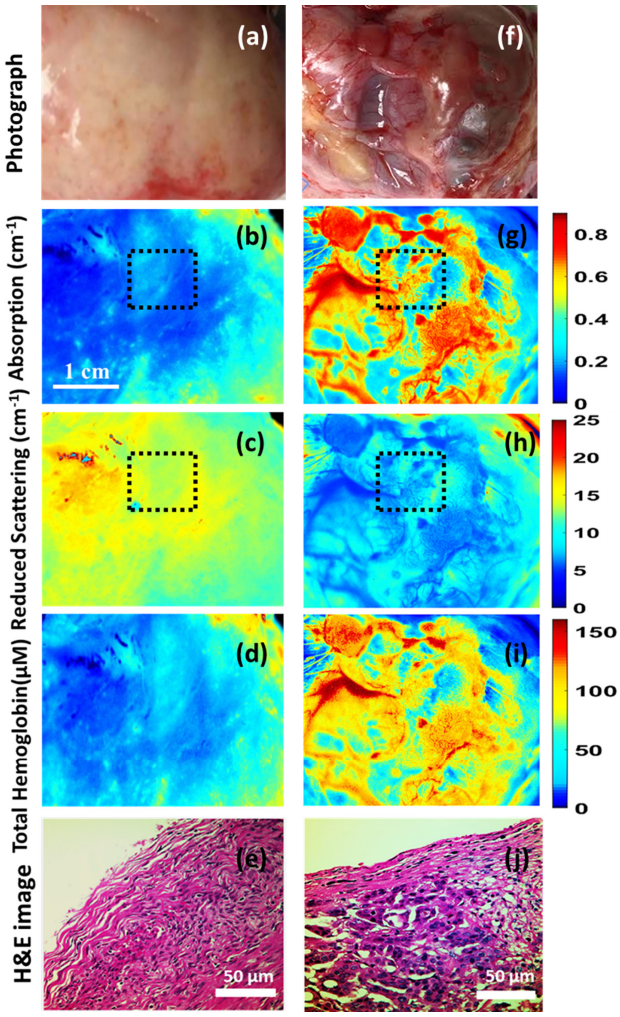

Fig. 2. Color photograph, absorption, reduced scattering (530 nm), total hemoglobin map, H&E image from representative areas of a benign fibrothecoma (a-e) and a high-grade serous carcinoma (f-j); Black dashed area showing the ROI for feature selection.

Figure 2 shows the color photograph, absorption, and reduced scattering maps at 530 nm, total hemoglobin (HbT) as well as representative H&E-stained histology images from corresponding areas of a benign ovarian fibrothecoma (2a-2e) and a high-grade serous carcinoma (2f-2j) respectively. A fibrothecoma was chosen for comparison here because it represents a mass-forming process, potentially mimicking a malignancy, yet is benign. Six fallopian tubes (all normal) were also imaged; however, due to lack of any malignant fallopian tubes in the current sample pool, fallopian tubes were not included for classification in this study.

It was observed that the malignant ovaries had significantly higher total hemoglobin as well as lower scatter amplitude and slope, as shown in Fig. 3. This may be due to increased

Biomedical Optics EXPRESS

angiogenesis and lack of elastic scatterers such as stromal collagen in the malignant ovarian tissue compared to the non-cancerous ovaries, as evident in the H&E images from the imaging areas of benign and malignant ovaries in Fig. 2(e) and 2(j). Additionally, the absorption and scatter heterogeneity was also highest for the malignant group, signifying clustered, random distribution of micro vessels as well as scattered collagen distribution. The SD of the Gaussian fitting function was also found to be significantly lower for the malignant group as compared to the normal group. In terms of statistical significance, HbT was found to be the most important feature, followed by scatter slope, scatter amplitude, absorption heterogeneity, absorption SD, scatter heterogeneity and scatter SD. Oxygen saturation was not found to be a significant *ex vivo* feature ($p = 0.53$), which might be due to variations after resection, as reported by other researchers [13].

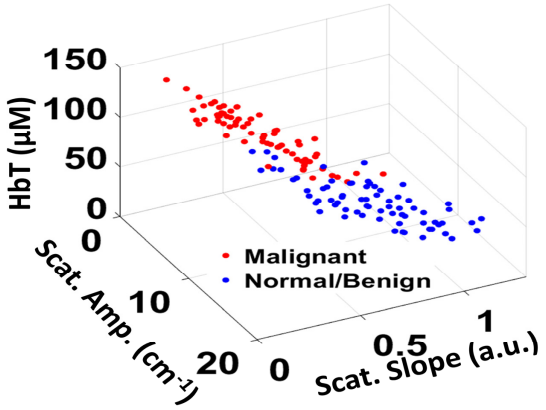

Fig. 3. Scatter plot of spectral features of Normal/Benign and Malignant ovaries.

A total of 53 independent ROIs (35 normal/benign, 18 cancer) were used for quantitative feature extraction. Figure 4 (a-g) show the boxplots of the seven features calculated from the spectral and spatial differences between the different types of ovarian tissue. Approximately two thirds of the data (30 ROIs, including 20 normal/benign, 10 cancer) were used for training and the rest were used for testing the logistic model. Figure 5 shows the ROC curves and AUC of the training and testing set. For the training set, we obtained sensitivity 97.69%, specificity 96.97%, PPV 96.21%, NPV 97.97% and AUC (95% confidence interval) of 0.985. For the testing set, we obtained sensitivity 94.06%, specificity 93.53%, PPV 92.23%, NPV 95.04% and AUC (95% confidence interval) of 0.938.

The current work improves on our previous SFDI ovary study in terms of multispectral information of important tissue chromophores, as well as reduction of overall size of the projection unit. However, the limited sample size ($n = 14$) remains a challenge, as well as lack of benign or malignant fallopian tubes in the current sample pool. This is of interest, as some recent research has indicated the fallopian tube as the potential site of origin for ovarian cancer [14]. Since the technology is best suited for assessing the surface of the ovary, it might have limited ability to detect small foci of invasion (i.e., malignancy) occurring at depth within a large ovarian mass. For translating this technology from bench to bedside, a fully hand-held multispectral SFDI projection and camera based system is currently being developed, which can be readily used by the surgeons in the operating room for quantitative evaluation of the ovarian and fallopian tube tissue surface, and reduce the risk of unnecessary surgeries.

Biomedical Optics EXPRESS

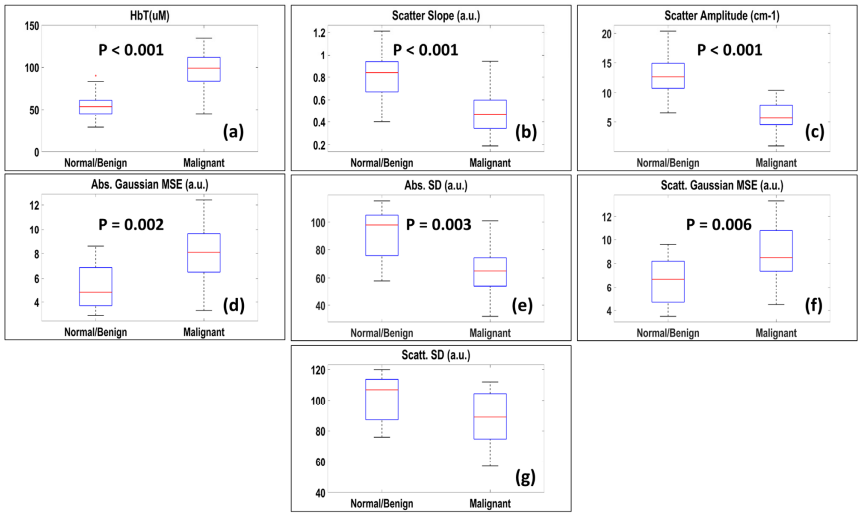

Fig. 4. Boxplots of (a) Total hemoglobin; (b) Scatter slope; (c) Scatter amplitude; (d) Absorption Gaussian MSE; (e) Absorption. SD; (f) Scatter Gaussian MSE; (g) Scatter SD.

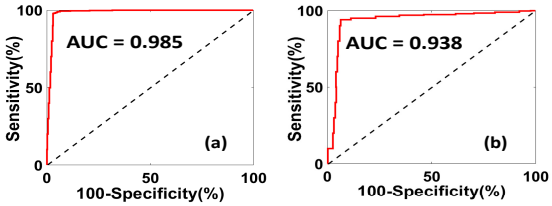

Fig. 5. ROC curves of (a) Training; (b) Testing.

4. Conclusions

In this study, a multispectral SFDI system was used for quantitative, wide-field evaluation of human ovarian tissues. 14 ovaries from 11 patients were imaged and based on the spectral and spatial differences in absorption and scattering properties of normal/benign and malignant ovaries, seven features were extracted from the SFDI images. Using a logistic regression model, sensitivity of 94.06%, specificity of 93.53%, PPV 92.23%, NPV 95.04% was obtained. The initial promising results indicate the prospect of using SFDI for intraoperative assessment of the ovarian tissue to avoid potentially unnecessary surgeries. Future studies will be concentrated on upgrading this technology from bench to bedside and building SFDI systems that can be readily used in the operating room.

Funding

National Institute of Health (NIH) (R01CA151570).

Acknowledgements

The authors would like to thank Dr. Andrea Hagemann and Dr. Katherine Fuh from the department of Obstetrics & Gynecology at Washington University School of Medicine for patient recruitment. The authors would also like to thank Ruth Holdener and Lynne Lippmann from Radiology and Gynecologic Oncology division at Washington University School of Medicine for helping with patient consent and study coordination.

Disclosures

The authors declare that there are no conflicts of interest related to this article.